

LA-UR-

*Approved for public release;
distribution is unlimited.*

Title:

Author(s):

Submitted to:



Los Alamos National Laboratory, an affirmative action/equal opportunity employer, is operated by the University of California for the U.S. Department of Energy under contract W-7405-ENG-36. By acceptance of this article, the publisher recognizes that the U.S. Government retains a nonexclusive, royalty-free license to publish or reproduce the published form of this contribution, or to allow others to do so, for U.S. Government purposes. Los Alamos National Laboratory requests that the publisher identify this article as work performed under the auspices of the U.S. Department of Energy. Los Alamos National Laboratory strongly supports academic freedom and a researcher's right to publish; as an institution, however, the Laboratory does not endorse the viewpoint of a publication or guarantee its technical correctness.

EVENT GENERATOR BENCHMARKING FOR PROTON RADIOGRAPHY APPLICATIONS

Stepan G. Mashnik, Richard E. Prael, Arnold J. Sierk
Los Alamos National Laboratory, Los Alamos, NM 87545, USA

Konstantin K. Gudima
Institute of Applied Physics
Academy of Science of Moldova, Kishinev, MD-2028, Moldova

Nikolai V. Mokhov
Fermi National Accelerator Laboratory, Batavia, IL 60510, USA

Abstract

We have benchmarked the QGSM code and event generators of the MARS and LAHET3 codes as potential candidates for high-energy programs to be used in simulations for the Proton Radiography (PRad) Project. We have compiled from the literature experimental data on spectra of particles emitted from proton-induced reactions at incident energies from 30 GeV to 70 GeV on different nuclei and have performed calculations for all reactions for which we found data with these three codes without any modifications and using only default parameters and standard inputs. Our results (514 plots) show that all three codes describe reasonably most of the studied reactions, though all of them should be further improved before becoming reliable tools for PRad. We present here our conclusions concerning the relative roles of different reaction mechanisms in the production of specific secondary particles. We comment on the strengths and weaknesses of QGSM, MARS, and LAHET3 and suggest further improvements to these codes and to other models.

Introduction

The process of determining the feasibility of Proton Radiography (PRad) [1-3] as the radiographic probe for the Advanced Hydrotest Facility as well as its design and operation require information about spectra of secondary particles produced by high energy protons interacting in the target and structural materials. Reliable models and codes are needed to provide such data. We studied the literature and chose three potential candidates for high-energy codes that may be used in simulations for PRad, namely the Quark-Gluon String Model (QGSM) as developed by Amelin, Gudima, and Toneev [4], the MARS code by Mokhov *et al.* [5], and a version of the Los Alamos National Laboratory (LANL) transport code LAHET [6], known as LAHET3 [7].

The energy of the proton beam at PRad is supposed to be about 50 GeV. Unfortunately, there are very few measurements of particle spectra for proton-induced reactions exactly at 50 GeV or very close energies. In fact, we found only one published work at 50 GeV, namely spectra of π^- and π^+ measured at 159° from $p(50 \text{ GeV}) + W$ published in Russian together with pion spectra for other energies and targets, in a Joint Institute for Nuclear Research (Dubna) Communication by Belyaev *et al.* [8].

With only a few data available at 50 GeV, we benchmarked QGSM, MARS, and LAHET3 against measured spectra of particles emitted from interaction of protons with energies 50 ± 20 GeV, *i.e.*, from 30 to 70 GeV, with all targets for which we found experimental data. Independently of how many spectra were measured in an experiment, we performed calculations with the standard versions of QGSM, MARS, and LAHET3 without any modifications or adjustments, using only default parameters in the input of codes, and calculated double differential cross sections at 0, 4.75, 9, 13, 20, 45, 60, 90, and 159 degrees, angle-integrated energy spectra, and mean multiplicities for emission of n, p, d, t, ^3He , ^4He , π^+ , π^- , K^+ , K^- , and \bar{p} for all cases listed below in Table 1. The next Section presents a brief description of the benchmarked codes, followed by results, discussion, and conclusions in the last two Sections.

Benchmarked Codes

QGSM: The core of the QGSM is built on a time-dependent version of the intranuclear cascade model developed at Dubna to describe both particle- and nuclei-induced reactions, often referred in the literature simply as the Dubna intranuclear Cascade Model (DCM) (see [9] and references therein). The DCM models interactions of fast cascade particles (“participants”) with nucleon spectators of both the target and projectile nuclei and includes interactions of two participants (cascade particles) as well. It uses experimental cross sections (or those calculated by the Quark-Gluon String Model for energies above 4.5 GeV/nucleon) for these elementary interactions to simulate angular and energy distributions of cascade particles, also considering the Pauli exclusion principle. When the cascade stage of a reaction is completed, QGSM uses the coalescence model described in [9] to “create” high-energy d, t, ^3He , and ^4He by final state interactions among emitted cascade nucleons, already outside of the colliding nuclei. After calculating the coalescence

stage of a reaction, the QGSM moves to the description of the last slow stages of the interaction, namely to preequilibrium decay and evaporation, with a possible competition of fission using the standard version of the Cascade Exciton Model (CEM) [10]. But if the residual nuclei have atomic numbers with $A \leq 13$, QGSM uses the Fermi break-up model to calculate their further disintegration instead of using the preequilibrium and evaporation models.

MARS: The MARS Monte-Carlo code system, being developed over 29 years, allows fast and reliable inclusive and exclusive simulation of three-dimensional hadronic and electromagnetic cascades in shielding, accelerator and detector components in the energy range from a fraction of an electron-volt up to about 100 TeV [5]. It is under continuous development. The reliable performance of the code has been demonstrated in numerous applications at Fermilab, CERN, KEK and other centers as well as in special benchmarking studies. Description of elastic and inelastic hN , hA , γA and νA cross sections is based on the newest compilations and parameterizations [11]. At high energies ($5 \text{ GeV} < E < 100 \text{ TeV}$), σ_{tot} , σ_{in} , σ_{prod} and σ_{el} are calculated in the framework of the Glauber multiple scattering theory with the σ_{hN} as an input. The nucleon density distribution in nuclei is represented as the symmetrized Fermi function with the parameters of [12] for medium and heavy nuclei ($Z > 10$) and the ones of [13] for $Z < 10$. Modern evaluated nuclear data as well as fitting formulae are used to simulate hadron-nucleus elastic scattering. For protons, nuclear, Coulomb elastic scattering, and their interference is taken into account. At $E > 5 \text{ GeV}$, a simple analytical description used in the code for both coherent and incoherent components of $d\sigma/dt$ is quite consistent with experiment. A version of the Cascade-Exciton Model of nuclear reactions [10] as realized in the code CEM95 [14] and containing also several recent refinements [15] is now implemented in the 1998 version of MARS [11] as default for $1\text{-}10 \text{ MeV} < E < 3\text{-}5 \text{ GeV}$. A set of phenomenological models, as described in Ref. [5, 16, 17], is used for inclusive production of secondary particles in hA , dA , γA and νA interactions at projectile energies from 5 GeV to 100 TeV. The 2001 version [11] of the MARS code was employed in the present benchmark.

LAHET3: LAHET is a Monte-Carlo code for the transport and interaction of nucleons, pions, muons, light ions, and antinucleons in complex geometry [6]; it may also be used without particle transport to generate particle production cross sections. LAHET allows one to choose one of several options for the Intra-Nuclear Cascade (INC) and fission models to be employed in calculations; it is widely used and well known in the applied nuclear physics community; therefore, we do not describe it here (a comprehensive description of LAHET may be found in [6] and references therein). The version of LAHET realized in the code LAHET3 [7] uses a version of the code FLUKA, known in the literature as FLUKA96 [19] to describe the first, INC stage of reactions, and its own Multistage Preequilibrium Model (MPM) [20] to describe the following intermediate preequilibrium stage, followed by evaporation/fission slow processes (or by the Fermi break-up model after the cascade instead of preequilibrium and evaporation/fission, if the residual nuclei have atomic numbers with $A \leq 13$ and for $14 \leq A \leq 20$ with excitation energy below 44 MeV), as described in [6, 7]. We mention again that only the high-energy event generator from FLUKA96 is employed here, as implemented in LAHET3; the de-

fault preequilibrium, evaporation and Fermi break-up models of LAHET3 are used for low energy nucleon and complex particle emission. More details and further references on LAHET3 with FLUKA96 can be found in [21].

Results and Discussion

Table 1 lists the cases we calculated with QGSM, MARS, and LAHET3, and provides references to experimental works where at least one spectrum of a secondary particle (from the ones listed in Introduction) was measured. A detailed report of the study containing 514 plots with spectra and multiplicities of secondary particles from reactions listed in Tab. 1 is now in preparation. Here, we present only our main conclusions and several

Table 1. Proton energy and target list covered by the present benchmark

T_p (GeV)	Nuclei	Measurements
30	${}^9\text{Be}$, ${}^{27}\text{Al}$	[8, 22–24]
47	${}^{12}\text{C}$	[8, 25]
50	${}^{184}\text{W}$	[8, 25]
51	${}^9\text{Be}$, ${}^{48}\text{Ti}$	[8, 25]
53	${}^{27}\text{Al}$	[8, 25]
54	${}^{96}\text{Mo}$	[8, 25]
70	${}^{12}\text{C}$, ${}^{27}\text{Al}$, ${}^{64}\text{Cu}$, ${}^{118}\text{Sn}$, ${}^{208}\text{Pb}$	[26–30]

examples of results from the study.

Our analyses have shown that all three codes tested here describe reasonably most of the secondary particle spectra. As a rule the higher the incident proton energy, the better the calculated spectra agree with experimental data. Several reaction mechanisms participate in the production of secondary nucleons and complex particles. These mechanisms are: 1) Fast INC processes; 2) preequilibrium emission from residual nuclei after the cascade stage of reactions; 3) evaporation of particles from compound nuclei after the preequilibrium stage, or from fission fragments, if the compound nucleus was heavy enough to undergo fission; 4) Fermi break-up of light excited nuclei formed after the cascade stage of reactions; 5) coalescence of complex particles by final state interactions among emitted cascade nucleons; 6) fast complex particle emission via knock out and pick up processes; 7) Multifragmentation of highly-excited residual nuclei after the INC. Their relative roles change significantly with the changing atomic mass number of the targets, and are different for different energies and angles of emission of secondary particles. Different codes describe these spectra better, worse, or do not describe them at all, depending of how these reaction mechanisms are (or are not) implemented into a specific code.

As an example, Fig. 1 shows spectra of p, d, t, and π^- emitted at 9.17 deg from the reaction $p(70 \text{ GeV}) + {}^{208}\text{Pb}$. Results for other reactions at 70 GeV are similar. One can see that all three codes describe the proton spectra well. The agreement for the pion spectra is not so good but is still reasonable, with some underestimation of the high-energy

tails of spectra by QGSM and some overestimation by MARS. Note that as the angle of pion emission changes the situation is reverses: we observe that most of the high-energy tails of pion spectra at 159 deg, and to a lesser extent at 90 deg, are over-predicted by LAHET3 and underestimated by MARS.

The situation with the deuteron and tritium spectra is quite different. We see that deuterons with momentum of up to about 15 GeV/c and tritium with momenta up to 19 GeV/c are emitted and measured in this particular reaction. Utilizing the coalescence mechanism for complex particle emission, QGSM is able to describe high-energy deuteron production, and agrees well with the measurement. LAHET3 does not consider the coalescence of complex particles and therefore describes emission of only evaporative and preequilibrium deuterons with momenta not higher than 1 GeV/c. MARS does not consider emission of complex particles at such high incident proton energies, therefore no d and t spectra by MARS are shown in Fig. 1.

For tritium, the situation is worse since LAHET3, as is the case of deuterons, describes only preequilibrium emission and evaporation of tritons with momenta not higher than 1 GeV/c and QGSM, even taking into account coalescence of tritium, describes emission of t from this reaction up to only 2.5 GeV/c while the experimental spectrum of t extends to 19 GeV/c. This deficiency can be understood by considering the coalescence mechanism: It is much more probable to emit two cascade nucleons with very similar momenta that can coalesce into a deuteron than to get three INC nucleons with very similar momenta that can coalesce into a triton. The experimental values of high-energy triton spectra are several orders of magnitude below the corresponding values of the deuteron spectra, and the statistics of our present QGSM simulation could be simply too small to get such high-energy tritium via coalescence. There is also a possibility that knock out processes of preformed clusters (or fluctuations of nuclear density, leading to “fluctons”) by bombarding protons are seen in these experimental d and t spectra, but are not taken into account by any of the tested codes, providing the observed difference in the t spectrum and less pronounced, in the d spectrum. A third possible mechanism of complex particle emission with greater than 1 GeV/c momenta would be multifragmentation of highly-excited residual nuclei after the INC. This mechanism is not taken into account by any of the tested codes and we cannot estimate its contribution.

Fig. 2 shows examples of π^+ spectra at 159 deg from 51 GeV proton collisions with ^9Be and ^{48}Ti . As already mentioned above for π^- , we see that LAHET3 overestimates the high-energy tails of pion spectra and MARS underestimates them a little. Similar results were obtained for other targets and incident proton energies.

Fig. 3 shows an example of how calculated proton spectra depend on the angle of emission, for the reaction $p(30 \text{ GeV}) + ^9\text{Be}$. We see that at 30 GeV, the agreement of calculated proton spectra with the data is not so good as we have in Fig. 1 for 70 GeV. The shapes and absolute values of proton spectra predicted by different codes depend significantly on the angle of detection, as does the agreement with the data. Similar results were obtained for other secondary particles and for other targets and incident energies.

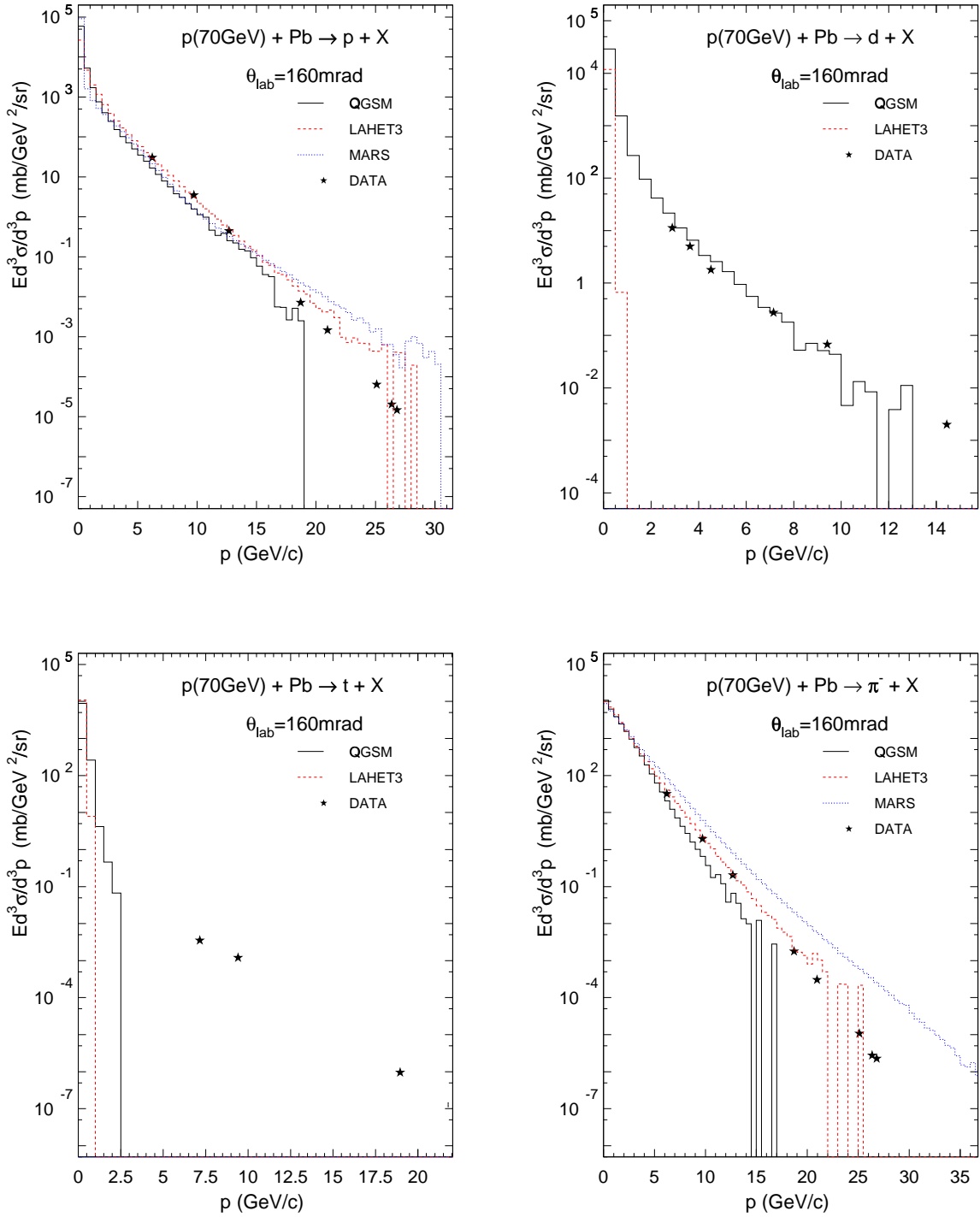


Figure 1. Invariant cross sections $Ed^3\sigma/d^3p$ for forward production of p, d, t, and π^- at 160 mrad (9.17 deg) as functions of particle momentum p from 70 GeV protons on ^{208}Pb . Experimental data for p and π^- are from Tab. 1 of Ref. [29] and for d and t, from Ref. [30]. Calculations by QGSMM, LAHET3, and MARS are shown as indicated in the legends.

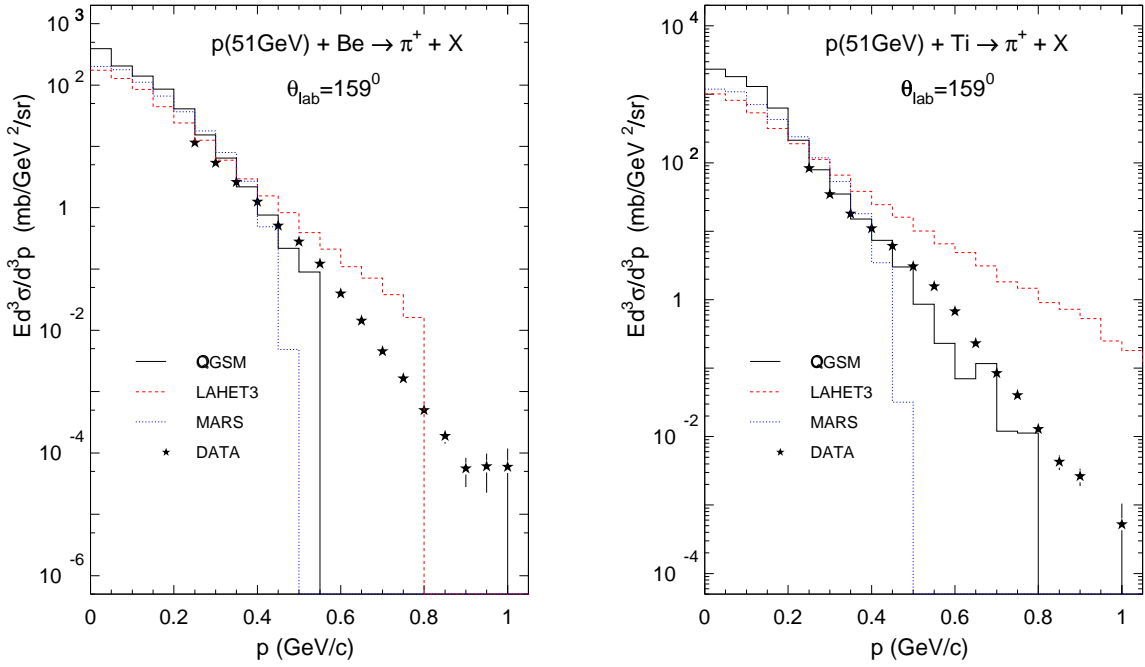


Figure 2. Invariant cross sections $Ed^3\sigma/d^3p$ for production of π^+ at 159 deg as functions of pion momentum p from 51 GeV protons on ^9Be and ^{48}Ti . Experimental data are by Belyaev *et al.* [8]. Calculations by QGSM, LAHET3, and MARS are shown as indicated in legends.

Fig. 4 shows an example of mean multiplicity of secondary n, p, d, and π^+ predicted by the tested codes for interaction of protons of about 50 GeV with different nuclei as functions of the mass number of targets. We see that predicted particle multiplicities differ significantly from each other, and the differences increase with increasing mass number of the target. The observed differences point to a quite significant difference in the treatment by the codes of the cascade stage of reactions (pions are emitted only at the cascade stage of reactions) and of the subsequent preequilibrium, evaporation, and Fermi break-up stages as well (we recall that at these incident energies MARS uses its own approximations for the total particle spectra without considering separately contributions from different mechanisms of nuclear reactions). These differences indicate that further experimental data are necessary at these incident proton energies and further development and improvement of the codes is required.

Further Work

Our study shows that all three codes describe reasonably well many of the secondary particle spectra analyzed here, though all of them should be further improved before becoming reliable tools for PRad.

For instance, we find that QGSM has some problems in a correct description of several pion spectra and does not describe sufficiently the high-energy tails of measured t and ^3He spectra. Nevertheless, QGSM is the only code tested here that accounts for coalescence of

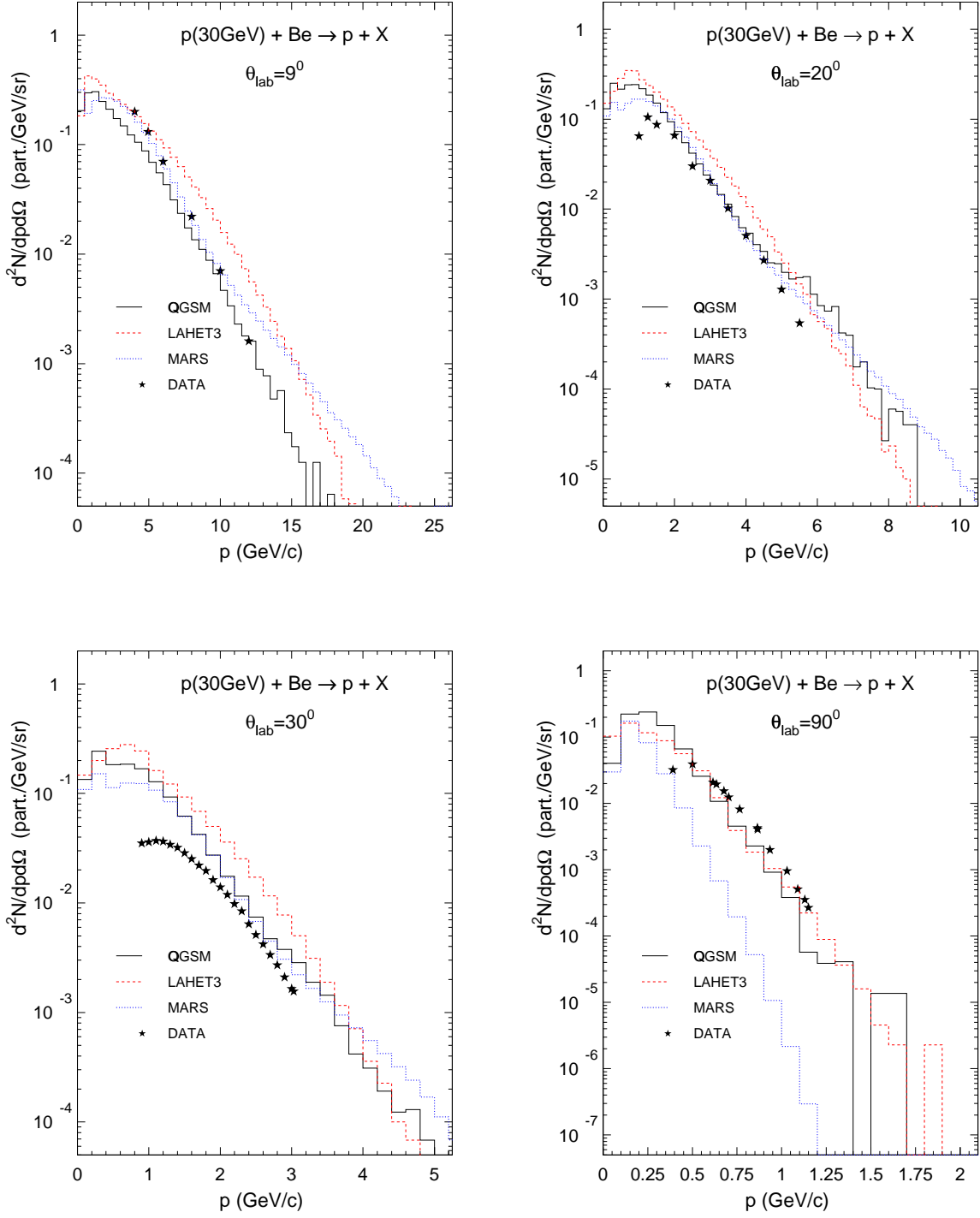


Figure 3. Momentum spectra of secondary protons from 30 GeV protons on Be. Experimental data at 9 and 20 degrees are taken from Fig. 1 of Baker *et al.* [22]; at 30 degrees, from Fig. 5 of Ref. [23]; and at 90 degrees, from Fig. 2 of Ref. [24]. Calculations by QGSM, LAHET3, and MARS are shown as indicated in legends.

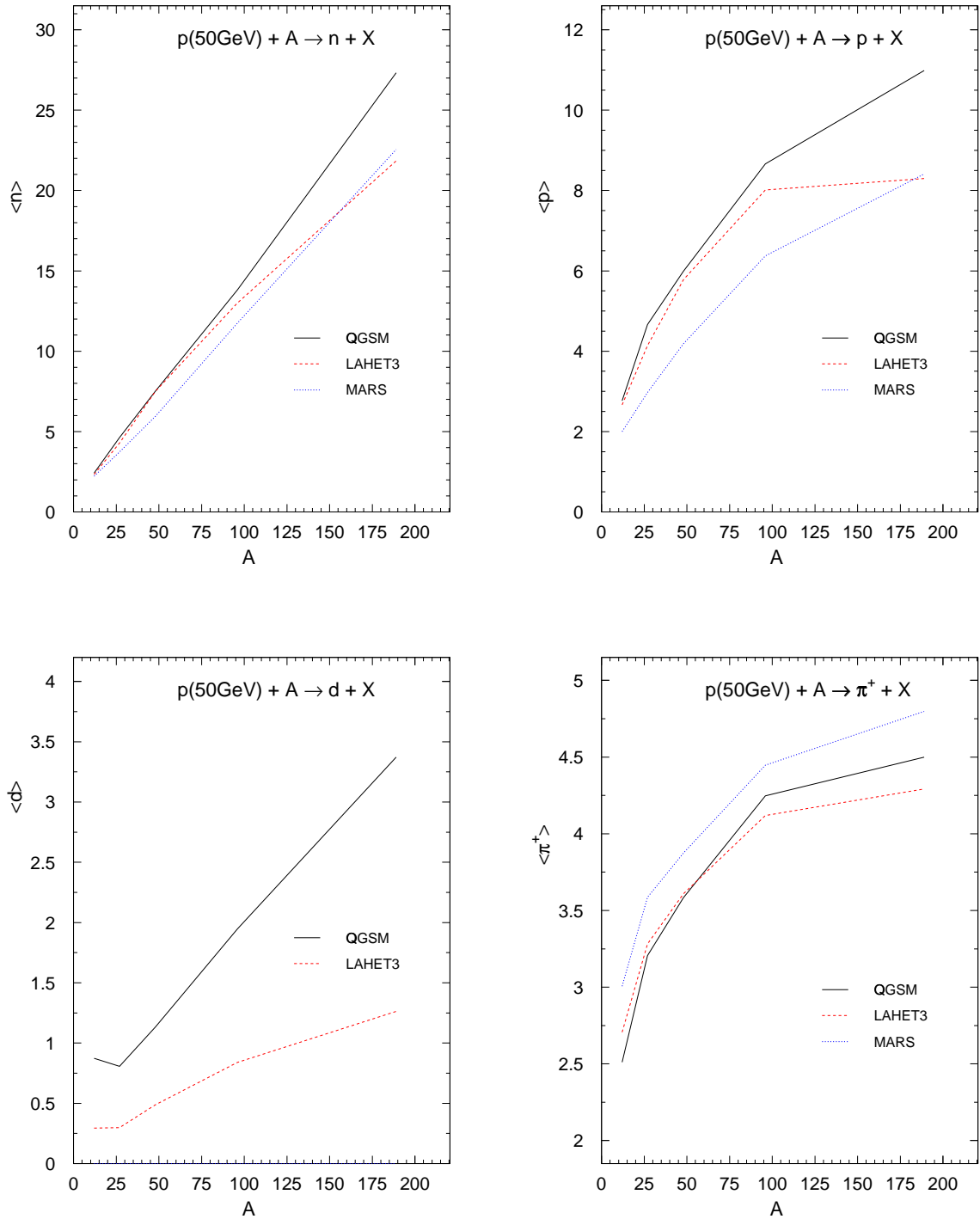


Figure 4. Predicted by QGSM, LAHET3, and MARS mean multiplicities of secondary n , p , d , and π^+ emitted from 50 GeV proton-induced reactions as functions the mass number of targets. Note that actual energies of incident protons in our calculations were 47 GeV for ^{12}C , 50 GeV for ^{184}W , 51 GeV for ^9Be and ^{48}Ti , 53 GeV for ^{27}Al , and 54 GeV for ^{96}Mo . (MARS does not calculate production of deuterons at these incident energies.)

complex particles from cascade nucleons and provides production of high-energy complex particles.

MARS overestimates the high-energy tails of some pion, kaon, and proton spectra at small angles (4.75° , 9° , and 13°) and underestimates them a little at large angles (90° and 159°). At these incident energies, MARS does not calculate complex particle production. However, MARS has one significant advantage in comparison with the two other codes: It is several orders of magnitude faster and requires almost no computing time, providing meanwhile reliable results for many applications.

LAHET3 overestimates the high-energy tails of practically all pion spectra at 159° and some nucleon and complex particle spectra in the preequilibrium energy region. It does not consider coalescence of complex particles and does not describe production of high-energy complex particles.

We observe also big differences between predicted high-energy tails of both neutron and proton spectra at 0° and for the mean multiplicities of almost all secondary particles, though no experimental data for these quantities are available at present for the reactions studied here.

We note that many of the problems we observe in our study for particular codes have already been solved, since all benchmarked event generators are under continuous development and improvement and all of them have been further improved in comparison with the versions we use in this study.

On the basis of QGSM, we have developed the Los Alamos version of the Quark-Gluon String Model code, LAQGSM [31]. LAQGSM differs from QGSM by replacing the preequilibrium and evaporation parts of QGSM described according to the standard CEM [10] with the new physics from CEM2k [32] and has a number of improvements and refinements in the cascade and Fermi break-up models. Originally, both QGSM and LAQGSM were not able to describe fission reactions and production of light fragments heavier than ^4He , as they had neither a high-energy-fission nor a fragmentation model. Recently, we addressed these problems [33] by further improving CEM2k and LAQGSM and by merging them with the Generalized Evaporation Model code GEM2 developed by Furihata [34]. The improved LAQGSM+GEM2 code describes both spectra of secondary particles and yields of produced nuclides much better than QGSM does; exemplary results by LAQGSM and further references may be found in [35].

The MARS code system is being continuously developed and improved. For instance, a new version of the code, MARS14(2002) was completed after we started the present work. It contains a large number of improvements and refinements and provides better results in comparison with the version used here. Recently, the authors of MARS started to develop new and better approximations for the double differential cross sections of inelastic hN and hA interactions. The new systematics allow to solve the mentioned above problems with the pion, kaon, and proton spectra at forward and large angles and describe the experimental data much better.

The FLUKA code has also been updated very significantly (see *e.g.*, [36] and references therein) since the version FLUKA96 was incorporated into LAHET3 as used here; no updated version is yet incorporated into LAHET.

Our study points to the importance of taking into account coalescence in high-energy complex-particles production. We find it appropriate and easy to implement these processes into MARS and LAHET, as well as into other codes that do not now consider coalescence.

We think that at such high incident energies, multifragmentation of highly-excited heavy nuclei may also be of significance and should be taken into account in these event generators and in other codes.

Acknowledgment

The study was supported by the U. S. Department of Energy and by the Moldovan-U. S. Bilateral Grants Program, CRDF Project MP2-3025.

References

- [1] Christopher L. Morris, “Proton Radiography for an Advanced Hybrotest Facility,” Los Alamos National Report LA-UR-00-5716, 2000; <http://lib-www.lanl.gov/la-pubs/00357005.pdf>.
- [2] H.-J. Ziock *et al.*, “The Proton Radiography Concept,” Los Alamos National Report LA-UR-98-1368, 1998; <http://lib-www.lanl.gov/la-pubs/00460235.pdf>;
J. F. Amann *et al.*, “High-Energy Test of Proton Radiography Concepts,” Los Alamos National Report LA-UR-97-1520, 1997; <http://lib-www.lanl.gov/cgi-bin/getfile?00366878.pdf>.
- [3] N. S. P. King *et al.*, “An 800-MeV Proton Radiography Facility for Dynamic Experiments,” *Nucl. Instr. Meth.* **A424** (1999) 84–91.
- [4] N. S. Amelin, K. K. Gudima, and V. D. Toneev, “Ultrarelativistic Nucleus-Nucleus Collisions in a Dynamical Model of Independent Quark-Gluon Strings,” *Sov. J. Nucl. Phys.* **51** (1990) 1093–1101 [*Yad. Fiz.* **51** (1990) 1730–1743];
N. S. Amelin, K. K. Gudima, and V. D. Toneev, “Further Development of the Model of Quark-Gluon Strings for the Description of High-Energy Collisions with a Target Nucleus,” *Sov. J. Nucl. Phys.* **52** (1990) 172–178 [*Yad. Fiz.* **52** (1990) 272–282];
N. S. Amelin, “Simulation of Nuclear Collisions at High Energy in the Framework of the Quark-Gluon String Model,” Joint Institute for Nuclear Research Report JINR-86-802, Dubna (1986).
- [5] N. V. Mokhov, “The MARS Code System User’s Guide,” Fermilab-FN-628 (1995);
N. V. Mokhov and O. E. Krivosheev, “MARS Code Status,” Fermilab-Conf-00/181 (2000); <http://www-ap.fnal.gov/MARS/>.

- [6] R. E. Prael and H. Lichtenstein, “User Guide to LCS: The LAHET Code System,” LANL Report No. LA-UR-89-3014, Los Alamos (1989); <http://www-xdiv.lanl.gov/XTM/lcs/lahet-doc.html>.
- [7] R. E. Prael, “Release of LAHETTM Version 3.00,” Los Alamos National Laboratory Research Note XCI-RN 98-10 (U), January 14, 1998; LA-UR-00-2116; R. E. Prael, “Release Notes for LAHET Code System with LAHETTM Version 3.16,” LANL Report LA-UR-01-1655, Los Alamos, 2001; <http://lib-www.lanl.gov/lapubs/00795117.pdf>.
- [8] I. M. Belyaev *et al.*, “The Cross Sections of π^+ - and π^- Production at an Angle 159° l.s. in Proton-Nuclear Interactions at the Energy of the Incident Protons from 15 to 65 GeV,” JINR Communication P1-89-112, Dubna, Russia (1989); part of the Be data from this report are available from the HEPDATA: REACTION DATA Database at the web page <http://cpt19.dur.ac.uk/hepdata/reac2.html>.
- [9] V. D. Toneev and K. K. Gudima, “Particle Emission in Light and Heavy-Ion Reactions,” *Nucl. Phys.* **A400** (1983) 173c–190c.
- [10] K. K. Gudima, S. G. Mashnik, and V. D. Toneev, “Cascade-Exciton Model of Nuclear Reactions,” *Nucl. Phys.* **A401** (1983) 329–361.
- [11] N. V. Mokhov, S. I. Striganov, A. Van Ginneken, S. G. Mashnik, A. J. Sierk, and J. Ranft, “MARS Code Development,” Fermilab-Conf-98/379 (1998); LANL Report LA-UR-98-5716 (1998); Eprint: **nucl-th/9812038**; *Proc. Fourth Int. Workshop on Simulating Accelerator Radiation Environments (SARE-4)*, Hyatt Regency, Knoxville, TN, September 13–16, 1998, edited by T. A. Gabriel, ORNL (1999), pp. 87–99.
- [12] G. D. Alkhozov, S. L. Belostotsky, and A. A. Vorobyov, “Scattering of 1 GeV Protons on Nuclei,” *Phys. Rep.* **42** (1978) 89–144; H. de Veries, C. W. de Jager, and C. de Vries, “Nuclear Charge-Density-Distribution Parameters from Elastic Electron Scattering,” *Atomic Data and Nuclear Data Tables* **36** (1997) 495–536.
- [13] V. V. Burov, D. N. Kadrev, V. K. Lukianov, and Yu. S. Pol, “Analysis of Charge-Density Distributions in Nuclei,” *Phys. At. Nucl.* **61** (1998) 525–532 [*Yad. Fiz.* **61** (1998) 595–602].
- [14] S. G. Mashnik, “User Manual for the Code CEM95,” JINR, Dubna (1995); OECD NEA Data Bank, Paris, France (1995); <http://www.nea.fr/abs/html/iaea1247.html>; RSIC-PSR-357, Oak Ridge, 1995.
- [15] S. G. Mashnik and A. J. Sierk, “Improved Cascade-Exciton Model of Nuclear Reactions”, Eprint: **nucl-th/9812069**; *Proc. Fourth Int. Workshop on Simulating Accelerator Radiation Environments (SARE-4)*, Hyatt Regency, Knoxville, TN, September 13–16, 1998, edited by T. A. Gabriel, ORNL (1999), pp. 29–51.
- [16] A. N. Kalinovskii, N. V. Mokhov, Yu. P. Nikitin, *Passage of High-Energy Particles through Matter*, AIP, NY, 1989.

- [17] N. V. Mokhov and S. I. Striganov, “Model for Pion Production in Proton-Nucleus Interactions”, Proc. of the Workshop on Physics at the First Muon Collider, Fermilab, November 1997, AIP Conf. Proc. No. 435, pp. 453–459; Fermilab-Conf-98/053, 1998.
- [18] J. Ranft, “Dual Parton Model at Cosmic Ray Energies,” *Phys. Rev.* **D51**, (1995) 64–85; Gran Sasso Report INFN/AE-97/45, 1997.
- [19] A. Fasso, A. Ferrari, J. Ranft, and P. R. Sala, “An Update About FLUKA,” *Proc. of the Second Workshop on Simulating Accelerator Radiation Environments (SARE-2), CERN, Geneva, October 9–11, 1996*, edited by G. R. Stevenson, Geneva, Switzerland (1997), pp. 158–170; more references and many details on FLUKA may be found at the Web page <http://pcfluka.mi.infn.it/>.
- [20] R. E. Prael and M. Bozoian, “Adaptation of the Multistage Preequilibrium Model for the Monte-Carlo Method (I),” LANL Report LA-UR-88-3238, Los Alamos (1988).
- [21] R. E. Prael, A. Ferrari, R. K. Tripathi, and A. Polanski, “Comparison of Nucleon Cross Section Parametrization Methods for Medium and High Energies,” LANL Report LA-UR-98-5813 (1998); <http://www-xdiv.lanl.gov/XCI/PEOPLE/rep/>; *Proc. Fourth Int. Workshop on Simulating Accelerator Radiation Environments (SARE-4), Hyatt Regency, Knoxville, TN, September 13–16, 1998*, edited by T. A. Gabriel, ORNL (1999), pp. 171–181.
- [22] W. F. Baker *et al.*, “Particle Production by 10–30 BeV Protons Incident on Al and Be,” *Phys. Rev. Let.* **7** (1961) 101–104.
- [23] A. Schwarzschild and Č. Zupančič, “Production of Tritons, Deuterons, Nucleons, and Mesons by 30-GeV Protons on Al, Be, and Fe Targets,” *Phys. Rev.* **129** (1962) 854–862.
- [24] V. L. Fitch, S. L. Meyer, and P. A. Piroué, “Particle Production at Large Angles by 30- and 33-BeV Protons Incident on Aluminum and Beryllium,” *Phys. Rev.* **126** (1962) 1849–1851.
- [25] O. P. Gavrishchuk *et al.*, “Charged Pion Backward Production in 15–65 GeV Proton-Nucleus Collisions,” *Nucl. Phys.* **A523** (1991) 589–596; the Be data from this paper are available from the HEPDATA: REACTION DATA Database at the web page <http://cpt19.dur.ac.uk/hepdata/react2.html>.
- [26] L. M. Barkov, *et al.*, “Production of Low-Energy Hadrons at Zero Angle in Proton-Nucleus Collisions at Energy 70 GeV,” *Sov. J. Nucl. Phys.* **35** (1982) 694–698 [*Yad. Fiz.* **35** (1982) 1186–1193].
- [27] L. M. Barkov, *et al.*, “Measurement of the Cross Sections for Production of Hadrons with Momentum up to 2 GeV/c in Proton-Nucleus Collisions at Energy 70 GeV,” *Sov. J. Nucl. Phys.* **37** (1983) 732–737 [*Yad. Fiz.* **37** (1983) 1232–1240].
- [28] V. V. Abramov *et al.*, “High P_{\perp} Hadron Production off Nuclei at 70 GeV,” *Z. Phys.* **C24** (1984) 205–215.

- [29] V. V. Abramov *et al.*, “Production of hadrons with Large P_{\perp} in Nuclei at 70 GeV,” *Sov. J. Nucl. Phys.* **41** (1985) 227–236 [*Yad. Fiz.* **41** (1985) 357–370]; Preprint IFVE-84-26, Serpukhov (1984); tabulated values are available in the HEPDATA: REACTION DATA Database at the web page <http://cpt19.dur.ac.uk/hepdata/react2.html>.
- [30] V. V. Abramov *et al.*, “Production of Deuterons and Antideuterons with Large p_{\perp} in pp and pA Collisions at 70 GeV,” *Sov. J. Nucl. Phys.* **45** (1987) 845–851 [*Yad. Fiz.* **45** (1987) 1362–1372]; Preprint IFVE-86-56, Serpukhov (1986); tabulated values are available in the HEPDATA: REACTION DATA Database at the web page <http://cpt19.dur.ac.uk/hepdata/react2.html>.
- [31] K. K. Gudima, S. G. Mashnik, and A. J. Sierk, “User Manual for the Code LAQGSM,” Los Alamos National Report LA-UR-01-6804, 2001.
- [32] S. G. Mashnik and A. J. Sierk, “CEM2k—Recent Developments in CEM,” *Proc. AccApp00 (Washington DC, USA)*, pp. 328–341, La Grange Park, IL, USA, 2001; Eprint: **nucl-th/0011064**; Mashnik S. G., and A. J. Sierk, “Recent Developments of the Cascade-Exciton Model of Nuclear Reactions, *Proc. ND2001 (Tsukuba, Japan)*, *J. Nucl. Sci. Techn.*, **Supplement 2**, 720–725, 2002; Eprint: **nucl-th/0208074**.
- [33] S. G. Mashnik, K. K. Gudima, and A. J. Sierk, “Merging the CEM2k and LAQGSM Codes with GEM2 to Describe Fission and Light-Fragment Production,” *Proc. SATIF-6 (SLAC, USA)*; LANL Report LA-UR-02-0608, Los Alamos, 2002; S. G. Mashnik, A. J. Sierk, and K. K. Gudima, “Complex-Particle and Light-Fragment Emission in the Cascade-Exciton Model of Nuclear Reactions,” *Proc. RPSD 2002 (Santa Fe, NM)*; LANL Report LA-UR-02-5185, Los Alamos 2002; Eprint: **nucl-th/0208048**.
- [34] S. Furihata, “Statistical Analysis of Light Fragment Production from Medium Energy Proton-Induced Reactions,” *Nucl. Instr. Meth.* **B171** (2000) 252–258; S. Furihata, “The Gem Code Version 2 Users Manual,” Mitsubishi Research Institute, Inc., Tokyo, Japan, 2001.
- [35] S. G. Mashnik, K. K. Gudima, I. V. Moskalenko, R. E. Prael, and A. J. Sierk, “CEM2k and LAQGSM as Event Generators for Space-Radiation-Shielding and Cosmic-Ray-Propagation Applications,” *Proc. Second World Space Congress, COSPAR 2002, Houston, TX, USA, October 10–19, 2002*; LA-UR-02-6558, Los Alamos (2002); Eprint: **nucl-th/0210065**; to be published in the journal *Advances in Space Research*.
- [36] A. Fasso, A. Ferrari, J. Ranft, and P. R. Sala, “FLUKA: Status and Prospective for Hadronic Applications,” invited talk in the *Proc. Monte-Carlo 2000 Conf., Lisbon, October 23–26, 2000*, A. Kling, F. Barao, M. Nakagawa, L. Tavora, P. Vaz eds., Springer-Verlag, Berlin pp. 955–960 (2001); more references and many details on FLUKA may be found on the Web page <http://www.fluka.org/>.